

Application of R1224yd(Z) as R245fa alternative for high temperature heat pump

Takenobu KAIDA^(a), Masato FUKUSHIMA^(b), Koichiro IIZUKA^(c)

^(a) Central Research Institute of Electric Power Industry (CRIEPI)
Yokosuka, 240-0196, Japan, kaida@criepi.denken.or.jp

^(b) AGC Inc., Ichihara, 290-8566, Japan

^(c) Kobe Steel, Ltd., Kako, 675-0155, Japan

ABSTRACT

This paper discusses the suitability of R1224yd(Z) as R245fa alternative for high temperature heat pump. A drop-in test was performed when R245fa was replaced with R1224yd(Z) in a commercialized high temperature heat pump for industrial use. The test was performed by just replacing the refrigerant without changing any other components. In addition, the compatibility data with refrigeration oil, O-ring and motor insulation were obtained. The drop-in test result indicates better performance than the predicted thermodynamic simulation. As for the compatibility with refrigeration oil, O-ring and motor insulation, there were no significant differences between R1224yd(Z) and R245fa. Overall, R1224yd(Z) can be used as R245fa alternative for high temperature heat pump because of its good thermodynamic and environmental properties.

Keywords: Drop-in, HFO, High Temperature, Industrial Application, Performance.

1. INTRODUCTION

Heat pumps are among the key technologies for primary energy saving and greenhouse gas reduction. They are presently used mainly on air-conditioning and hot water heater in residential and commercial sectors, and then are expected to spread to industrial heating processes. For expanding the heat pump application range, some high temperature heat pumps with supply temperatures more than 100°C have been commercialized and are expected to become increasingly developed in the coming years.

Many of the commercialized high temperature heat pumps are used R245fa as the refrigerant (Arpagaus et al., 2018). However, R245fa has a high Global Warming Potential (GWP) of 858 and will be phased down in the foreseeable future. As the alternative refrigerant with lower GWP, R1224yd(Z) have been developed (Fukushima, 2015).

This paper discusses the suitability of R1224yd(Z) as R245fa alternative for high temperature heat pump. A drop-in test was performed when R245fa was replaced with R1224yd(Z) in a commercialized high temperature heat pump for industrial use. In addition, the compatibility data with refrigeration oil, O-ring and motor insulation were obtained.

2. CHARACTERISTICS OF R1224YD(Z)

2.1. Physical Properties

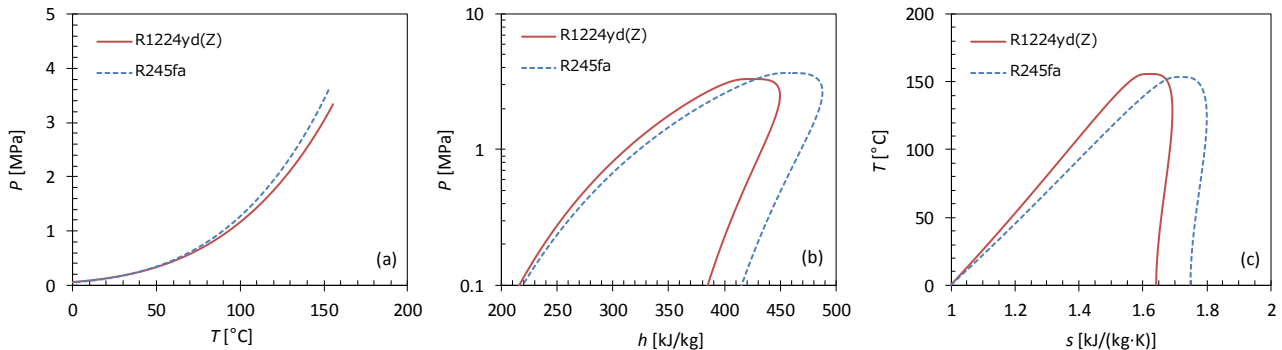
The physical properties of R1224yd(Z) is shown in Table 1 compared to R245fa. The normal boiling point and critical temperature of R1224yd(Z) are very close to the R245fa values, which implies that the thermodynamic performances would be similar. R1224yd(Z) is classified as A1 in ASHRAE Standard 34 safety group classification, which indicates low-toxicity and non-flammability. Ozone Depletion Potential (ODP) is 0.00023 and Global Warming Potential (GWP) is only 0.88 (Tokuhashi et al., 2018), which indicates that R1224yd(Z) is environmental-friendly refrigerant.

Table 1: Physical properties of R1224yd(Z) and R245fa

	R1224yd(Z)	R245fa
Molecular Formula	CF ₃ CF=CHCl	CHF ₂ CH ₂ CF ₃
Molar mass [g/mol]	148.49	134.05
Normal Boiling Point [°C]	14.62	15.05
Critical Temperature [°C]	155.54	153.86
Critical Pressure [MPa]	3.34	3.65
OEL [ppm]	1,000	300
Flammability Range [%]	None	None
ASHRAE Safety Classification	A1	B1
ODP	0.00023	0
GWP (AR5)	0.88	858

Figure 1 (a) compares the saturated vapor pressure of R1224yd(Z) to R245fa. The saturated vapor pressure of R1224yd(Z) is very close to the R245fa value at low temperature region but becomes somewhat lower at higher temperature. This implies that the use of R1224yd(Z) in high temperature heat pump at a given operating temperatures would enable lower pressure ratio operation.

Figure 1 (b) and (c) show the comparisons of pressure-enthalpy diagram and temperature-entropy diagram, respectively. R1224yd(Z) latent heat are smaller than the R245fa value. Similarly to R245fa, R1224yd(Z) shows a saturated vapor line with a positive slope ($dT/ds > 0$, except near the critical point). In the case of ideal compression, namely isentropic process, discharge superheat would be smaller than suction superheat. As a result, for preventing wet fluid compression and compressor damage, high temperature heat pump cycle with R1224yd(Z) would require sufficient superheat at the compressor inlet to ensure dry compression.

**Figure 1: Comparison of (a) P-T, (b) P-h, (c) T-s diagrams**

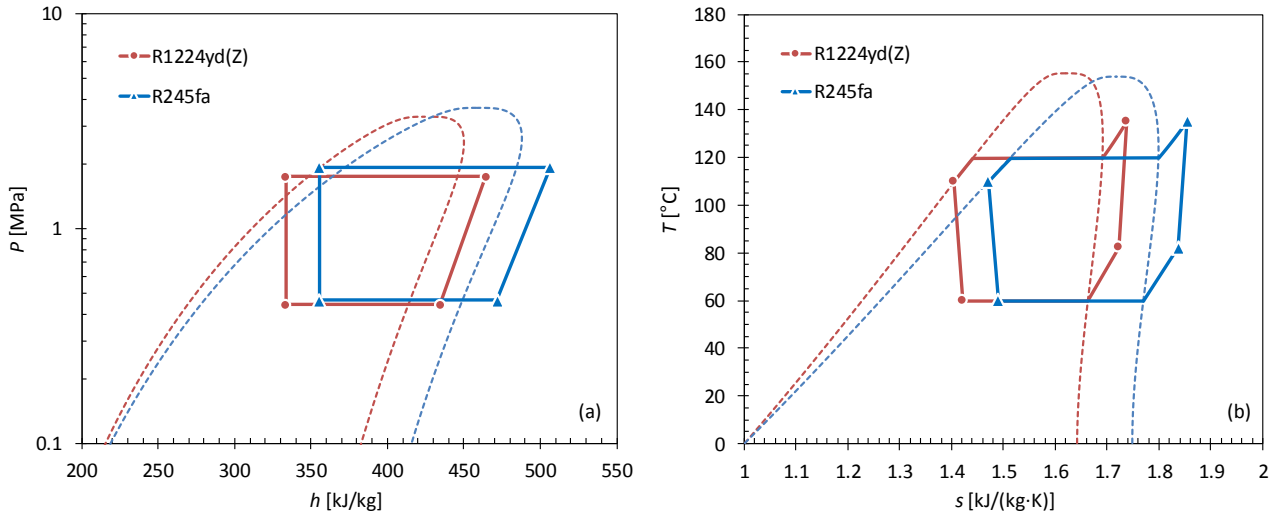
2.2. Predicted Thermodynamic Performance

The theoretical refrigerant cycle of R1224yd(Z) was calculated compared to R245fa refer to REFPROP program (Lemmon et al., 2018). The prediction was performed for simple heat pump cycle under the following conditions; condenser saturation temperature $T_{\text{cnd}} = 120^{\circ}\text{C}$, evaporator saturation temperature $T_{\text{evp}} = 60^{\circ}\text{C}$, discharge superheat $\Delta T_{\text{sh,d}} = 15 \text{ K}$, subcooling $\Delta T_{\text{sc}} = 10 \text{ K}$, compressor adiabatic efficiency $\eta_{\text{ad}} = 0.8$. This indicates that it is assumed that compressor, condenser and evaporator have the same performance between R1224yd(Z) and R245fa.

Table 2 and Figure 2 show the results. The coefficient of performance for heating, COP , with R1224yd(Z) would be similar to with R245fa. However, the volumetric heating capacity, VHC , with R1224yd(Z) would be 8% lower than with R245fa.

Table 2: Predicted thermodynamic performance of theoretical heat pump cycle $(T_{\text{cnd}} = 120^{\circ}\text{C}, T_{\text{evp}} = 60^{\circ}\text{C}, \Delta T_{\text{sh,d}} = 15 \text{ K}, \Delta T_{\text{sc}} = 10 \text{ K}, \eta_{\text{ad}} = 0.8)$

	R1224yd(Z)	R245fa
Suction Pressure P_s [MPa]	0.44	0.46
Discharge Pressure P_d [MPa]	1.75	1.93
Pressure Ratio P_d/P_s [-]	3.97	4.17
Coefficient of Performance for Heating COP [-]	4.38	4.36
Volmetric Heating Capacity VHC [MJ/m ³]	3.21	3.49

**Figure 2: Comparison of (a) P-h, (b) T-s diagrams in predicted thermodynamic performance**

3. PERFORMANCE EVALUATION

For surveying the actual performance including compressor, condenser and evaporator performances, a drop-in test was performed when R245fa was replaced with R1224yd(Z) in a commercialized high temperature heat pump for industrial use.

3.1. Test Method

A commercialized high temperature heat pump, HEM-HR115, which is the heat pump unit of SGH165, was used for the drop-in test. Originally, a mixture of R245fa and R134a was used as the refrigerant for HEM-HR115 (Iizuka and Maeda, 2011). In order to simply compare R1224yd(Z) to R245fa, the experimental tests were performed with pure R245fa and pure R1224yd(Z).

The test was performed with the HEM-HR115 installed at the large capacity heat pump evaluating apparatus in Central Research Institute of Electric Power Industry (Kaida et al., 2015). The apparatus can control the heat source water temperature from 10 to 90°C, simulating warm water effluents over a wide temperature range. The apparatus also can control the heat sink water or steam temperature up to 200°C.

Figure 3 shows the schematic cycle diagram of the test equipment, which is composed of a single-stage twin-screw compressor, a condenser, an evaporator, an internal heat exchanger, an economizer, a main expansion valve and an economizer expansion valve. All heat exchangers are plate type and two expansion valves are electronic automatic type. The same refrigerant weight of 140 kg was charged. Each of the inlet-outlet water temperatures, T_{c1} , T_{c2} , T_{h1} , T_{h2} , each of the water flow rates, V_c , V_h , and the power consumption, W were measured for evaluating the heating capacity, Q_h , and coefficient of performance, COP_h . The refrigerant pressures, P_s , P_d , P_{eco} , and the refrigerant temperatures, T_{r1} - T_{r9} , were also measured for reference.

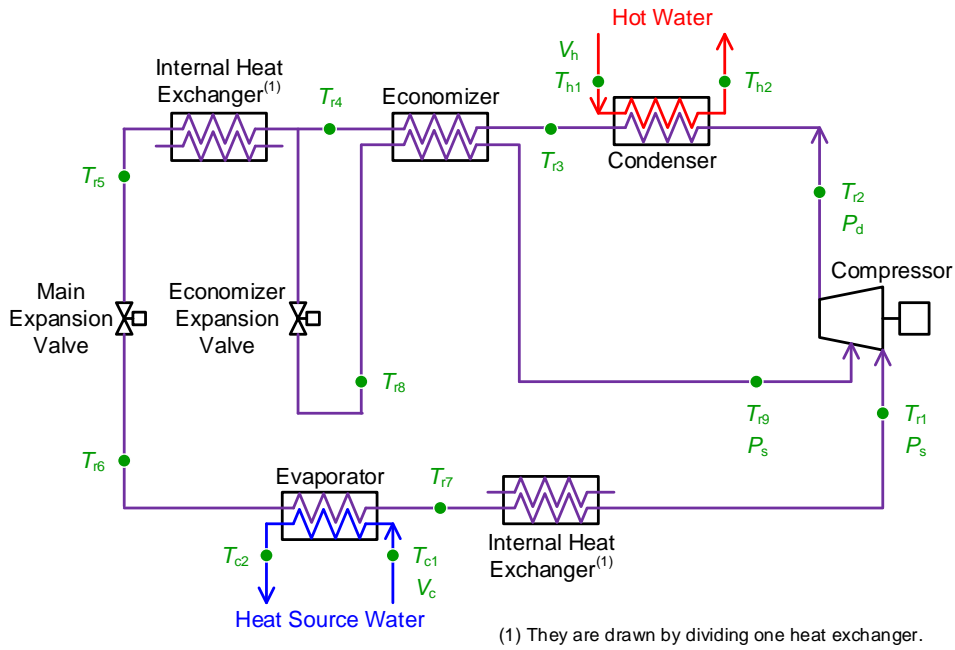


Figure 3: Schematic diagram of test equipment

Table 3 shows the test conditions. The test was performed in the compressor rotational speed fixed state to 100% with a difference of 5 K between outlet water temperature and inlet water temperature. The performances are evaluated under the same discharge superheat by controlling the main expansion valve. The economizer expansion valve was open and controlled at the economizer outlet superheat of about 20 K in Case 1, whereas was closed in Case 2 and Case 3.

Table 3: Test conditions

($\Delta T_c = T_{c1} - T_{c2} = 5$ K, $\Delta T_c = T_{c1} - T_{c2} = 5$ K, Compressor rotational speed = 100%)

	T_{c1} [°C]	T_{h2} [°C]	$\Delta T_{Sh,d}$ [K]	Economizer
Case 1	70	115	15	Open
Case 2	70	95	25	Closed
Case 3	50	95	27	Closed

3.2. Test Results

Figure 4 shows the test results as the relative value of R1224yd(Z) to R245fa. The COP_h of R1224yd(Z) was nearly equal to or higher than the R245fa value. The Q_h of R1224yd(Z) was nearly equal to or smaller than the R245fa value. These indicate better performances than predicted. Figure 5-7 show the comparisons of cycle diagrams. In all the case, the temperature lift, $T_{cnd} - T_{evp}$, with R1224yd(Z) was decreased by 3-5%. This would be one reason for the higher COP_h .

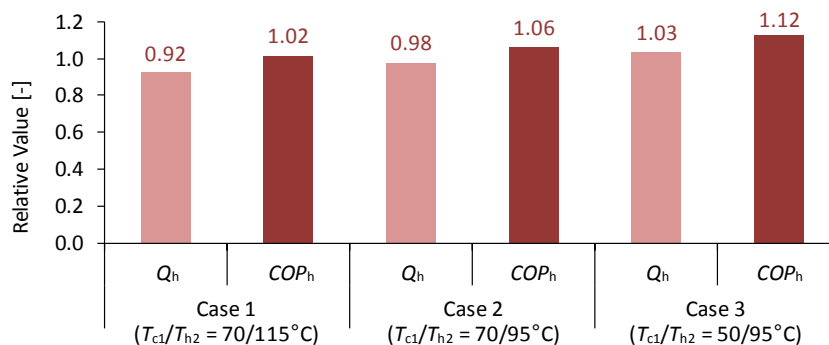


Figure 4: Actual performance of R1224yd(Z) relative to R245fa

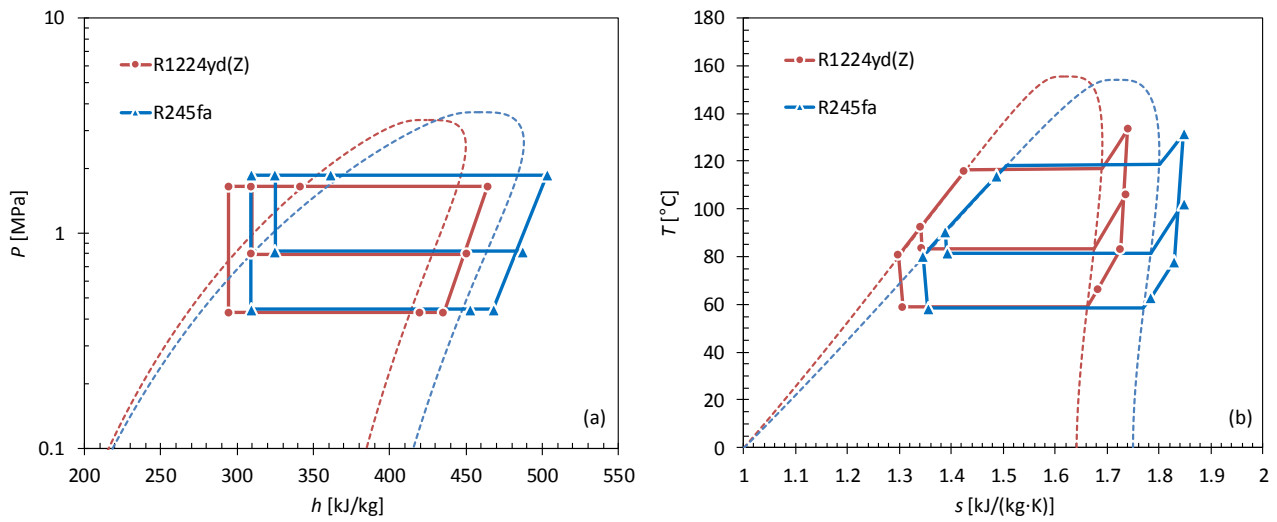


Figure 5: Comparison of (a) P-h, (b) T-s diagrams in actual performance ($T_{c1}/T_{h2} = 70/115^{\circ}\text{C}$)

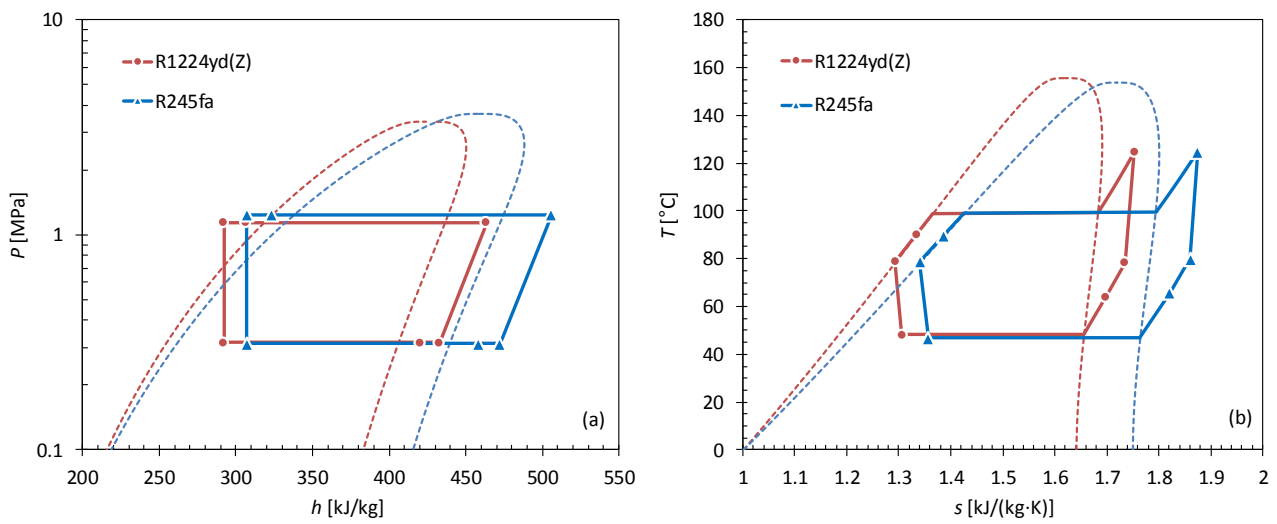


Figure 6: Comparison of (a) P-h, (b) T-s diagrams in actual performance ($T_{c1}/T_{h2} = 70/95^{\circ}\text{C}$)

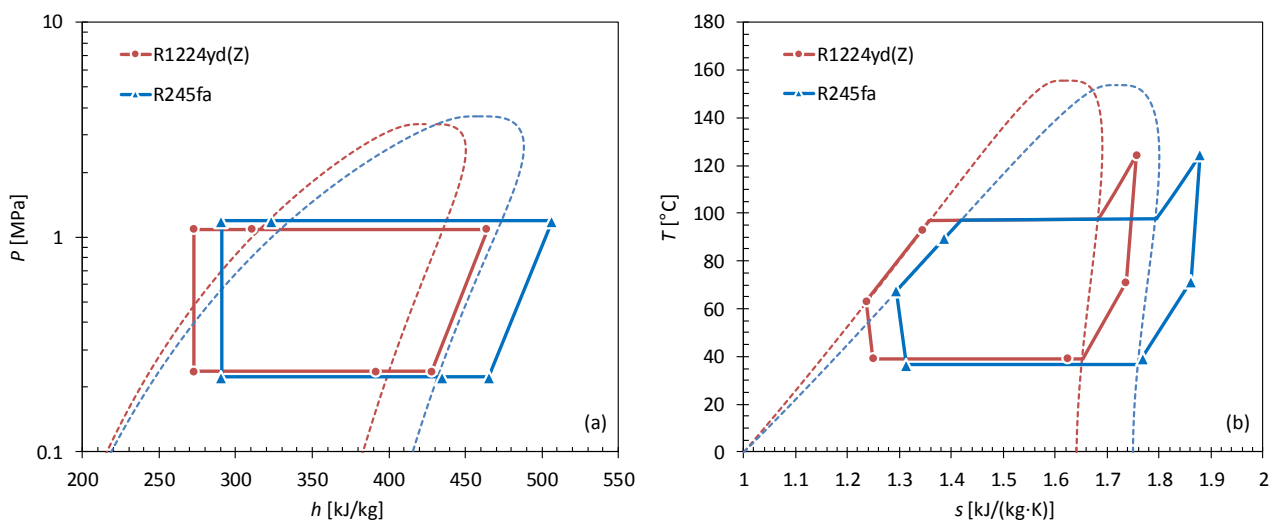


Figure 7: Comparison of (a) P-h, (b) T-s diagrams in actual performance ($T_{c1}/T_{h2} = 50/95^{\circ}\text{C}$)

3.3. Discussion

It cannot be explained only decreasing the temperature lift about the reason for the higher COP_h . Other reason for the higher COP_h is discussed. The compressor adiabatic efficiency has the maximum value at the pressure ratio of around 3 (Iizuka, 2014). In all the cases, by decreasing the pressure ratio, the compressor adiabatic efficiency of R1224yd(Z) would be larger than the R245fa value. This also results in the higher COP_h .

Next, the reason for the more Q_h than predicted is discussed. Although the heating effect of R1224yd(Z) was smaller than the R245fa value due to the smaller latent heat by 13-16%, the refrigerant flow rate of R1224yd(Z) was larger than the R245fa value by 6-23%. It is considered that the increase of refrigerant flow rate would moderate the decrease of heating capacity. Moreover, when the effect of increasing refrigerant flow rate was greater, the Q_h of R1224yd(Z) could be larger than the R245fa value.

The increase of refrigerant flow rate also leads to the enhancement of condensation and evaporation heat transfer coefficient. This would one reason for decreasing the temperature lift. Regarding transport properties, both liquid thermal conductivity and liquid viscosity of R1224yd(Z) is smaller than the R245fa value. The decrease degree is more of liquid viscosity. As a result, the heat transfer might be also enhanced from the viewpoint of transport properties.

4. CHEMICAL STABILITY AND COMPATIBILITY

The chemical stability of R1224yd(Z) with refrigerant oils, naphthene, alkylbenzene (AB) and polyolester (POE), had been evaluated (Fukushima, 2015, Soga et al., 2017). In this study, the chemical stability of R1224yd(Z) with the polyalkylene glycol (PAG) used in HEM-HR115 was tested. The compatibility of R1224yd(Z) with O-ring and motor insulation material was also tested.

4.1. Chemical Stability with Refrigerant Oil

The chemical stability of R1224yd(Z) with a PAG oil in the presence of metals was tested by sealed tube testing compared to R245fa. Each tube was prepared at 60 g refrigerant and 60 g oil, and included the three metal catalysts representing the system materials of construction; steel (SS), copper (Cu) and aluminium (Al). Each tube was aged in a heated oven at 150°C for 14 days.

The refrigerant purity was measured by gas chromatography analysis. The acidity of refrigerant was measured by alkalimetric determination (minimum limit of detection: 0.2 ppm). The concentration of fluoride ion (F) and chloride ion (Cl) was measured by ion chromatography (minimum limit of detection: 0.2 ppm). These can be interpreted as indicators of the degree of degradation. Moreover, the acid number of oil was measured by titration (minimum limit of detection: 0.01 mgKOH/g). The color of oil was also measured. These can be interpreted as indicators of the degree of reactivity. Furthermore, the weight change of each metal was measured.

Table 4: Chemical stability of R1224yd(Z) and R245fa with PAG oil in the presence of metals
(Temperature: 150°C, Duration: 14days)

		R1224yd(Z)	R245fa
Refrigerant	Purity change [%]	99.8 → 99.5	99.9 → 99.9
	Acidity [ppm]	< 0.2	< 0.2
	F [ppm]	< 0.2	< 0.2
	Cl [ppm]	< 0.2	< 0.2
Oil	Acid number [mgKOH/g]	0.05	0.03
	Color of oil (ASTM)	L0.5	L0.5
Metal	SS weight change [mg]	< 0.01	< 0.01
	Cu weight change [mg]	< 0.01	< 0.01
	Al weight change [mg]	< 0.01	< 0.01

Table 4 shows the results. Although the acid number and the color of the PAG oil with R1224yd(Z) was slightly larger than the R245fa value, there were no significant differences between R1224yd(Z) and R245fa.

4.2. Compatibility with O-ring and motor insulation material

The compatibility of R1224yd(Z) with two types of O-rings, hydrogenated-nitrile-butadiene rubber (HNBR) and ethylene-propylene-diene rubber (EPDM), and motor insulation material was tested by sealed tube testing compared to R245fa. Each tube was prepared at 80 g refrigerant and included each material. Each tube was aged in a heated oven at 150°C for 7 days. The refrigerant purity, the acidity of refrigerant, and the concentration of fluoride ion and chloride ion were measured. In addition, the weight change of each material was measured. Regarding O-rings, the wire diameter change and volume change were also measured.

Table 5 and Table 6 show the results. As shown in Table 5, both R1224yd(Z) and R245fa made O-rings expand slightly. The degrees of expansion were the same level. The expansion change rate of HNBR was larger than the EPDM value regardless of refrigerants. As shown in Table 6, both R1224yd(Z) and R245fa made motor insulation material heavy slightly. The degrees of weight change were the same level. As a result, there were no significant differences between R1224yd(Z) and R245fa.

Table 5: Compatibility of R1224yd(Z) and R245fa with O-ring
(Temperature: 150°C, Duration: 7days)

		R1224yd(Z)		R245fa	
Refrigerant	Purity change [%]	99.8→99.5	99.8→99.5	99.9→99.9	99.9→99.9
	Acidity [ppm]	< 0.2	< 0.2	< 0.2	< 0.2
	F [ppm]	0.2	< 0.2	< 0.2	< 0.2
	Cl [ppm]	< 0.2	< 0.2	< 0.2	< 0.2
O-ring	Type	HNBR	EPDM	HNBR	EPDM
	Wire diameter change [%]	3.3	1.3	4.3	0.7
	Volume change [%]	9.6	3.6	14.4	2.5
	Weight change [%]	13.7	7.2	16.9	2.8

Table 6: Compatibility of R1224yd(Z) and R245fa with motor insulation material
(Temperature: 150°C, Duration: 7days)

		R1224yd(Z)	R245fa
Refrigerant	Purity change [%]	99.8 → 99.7	99.9 → 99.9
	Acidity [ppm]	< 0.2	< 0.2
	F [ppm]	< 0.2	< 0.2
	Cl [ppm]	< 0.2	< 0.2
Motor insulation material	Weight change [%]	0.54	0.63

5. CONCLUSIONS

In order to evaluate the suitability of R1224yd(Z) as R245fa alternative for high temperature heat pump, a drop-in test with a commercialized industrial heat pump was performed. The test result indicates better performance than the predicted thermodynamic simulation. As this reason, (1) the enhancement of compressor adiabatic efficiency by decreasing pressure ratio, (2) the increase of heating capacity by increasing refrigerant mass flow rate, (3) the decrease of temperature lift by the enhancement of condensation and evaporation heat transfer coefficient due to increasing refrigerant mass flow rate and decreasing liquid viscosity, are considered. The heat transfer characteristics of R1224yd(Z) compared to R245fa needs to be examined further.

In addition, the chemical stability of R1224d(Z) with PAG oil in the presence of metals and the compatibility of R1224yd(Z) with O-ring and motor insulation were tested compared to R245fa. There were no significant differences between R1224yd(Z) and R245fa.

Overall, R1224yd(Z) can be used as R245fa alternative for high temperature heat pump because of its good thermodynamic and environmental properties.

NOMENCLATURE

AB	alkylbenzene	ad	adiabatic
c	cooling, heat source water	cnd	condenser
<i>COP</i>	coefficient of performance [-]	<i>VHC</i>	volumetric heating capacity [MJ/m ³]
d	discharge	eco	evaporator
EPDM	ethylene-propylene-diene rubber	evp	evaporator
h	heating, hot water	GWP	global warming potential
<i>h</i>	specific enthalpy [kJ/kg]	HNBR	hydrogenated-nitrile-butadiene rubber
ODP	ozone depletion potential	<i>P</i>	pressure [MPa]
PAG	polyalkylene glycol	POE	polyoester
Q	capacity [kW]	r	refrigerant
s	suction	s	specific entropy [kJ/(kg·K)]
sc	subcooling [K]	sh	superheat [K]
<i>T</i>	temperature [°C]	<i>V</i>	flow rate [m ³ /s]
<i>W</i>	electric power consumption [kW]	η	efficiency [-]

REFERENCES

- Arpagaus, C., Bless, F., Uhlmann, M., Schiffmann, J., Bertsch, S., 2018. High temperature heat pumps: Market overview, state of the art, research status, refrigerants, and application potentials. *Energy* 152, 985-1010.
- Kaida, T., Sakuraba, I., Hashimoto, K., Hasegawa, H., 2015. Experimental performance evaluation of heat pump-based steam supply system. *Proceedings of 9th International Conference on Compressors and their Systems*, London, 077.
- Fukushima, M., 2015. Development of low-GWP alternative refrigerants. *Proceedings of JSRAE Annual Conference*, Tokyo, D332. [in Japanese]
- Fukushima, M., 2018. Next generation low-GWP refrigerants “AMOLEA™.” *Proceeding of JRAIA International Symposium*, Kobe, 319-323.
- Iizuka, K., Maeda, M., 2011. Development of high efficiency steam supply systems “Steam Grow Heat Pump.” *Mechanical Engineering Congress*, Tokyo, W091008. [in Japanese]
- Iizuka, K., 2014. High efficiency steam supply systems using by heat pump cycle. *JSRAE Journal* 89 (1039), 13-18.
- Lemmon, E., Bell, I., Huber, M., McLinden, M., 2018. Reference Fluid Thermodynamic and Transport Properties Database (REFPROP): Version 10, National Institute of Standards and Technology (NIST).
- Soga, T., Hayamizu, H., Fukushima, M., 2017. Compatibility of low-GWP refrigerant HCFO-1224yd(Z). *Proceedings of JSRAE Annual Conference*, Tokyo, F312. [in Japanese]
- Tokuhashi, K., Uchimar, T., Takizawa, K., Kondo, S., 2018. Rate constants for the reactions of OH radical with the (E)/(Z) isomers of CF₃CF=CHCl and CHF₂CF=CHCl. *The Journal of Physical Chemistry A* 122, 3120-3127.